

## Supplementary Information

### Multifunctional Composite Films with Vertically Aligned ZnO Nanowires by Leaching-enabled Capillary Rise Infiltration

Hong Huy Tran,<sup>a</sup> R. Bharath Venkatesh,<sup>b</sup> Youngjin Kim,<sup>a</sup>

Daeyeon Lee\*<sup>b</sup> and David Riassetto\*<sup>a</sup>

<sup>a</sup> Univ. Grenoble Alpes, CNRS, Grenoble INP (Institute of Engineering Univ. Grenoble Alpes), LMGP, 38000 Grenoble, France

<sup>b</sup> Department of Chemical and Biomolecular Engineering,  
University of Pennsylvania, Philadelphia, Pennsylvania 19104, USA

\* Corresponding authors: [daeyeon@seas.upenn.edu](mailto:daeyeon@seas.upenn.edu)

[david.riassetto@grenoble-inp.fr](mailto:david.riassetto@grenoble-inp.fr)

#### Table of Contents

**Fig. S1.** Statistical analysis of the morphology of ZnO NWs.

**Fig. S2.** Top-view SEM image of ZnO NW.

**Fig. S3.** Schematic illustration and SEM images showing the LeCaRI process in the inverted bilayer to fabricate nanocomposite films with vertically aligned ZnO NWs.

**Fig. S4.** Optical microscope images of ZnO NWs, NCFs-10s@RT, and NCFs-24h@150 °C.

**Fig. S5.** EDS profile of ZnO NWs and nanocomposite films.

**Fig. S6.** Raman spectra of glass, ZnO NWs, PDMS, and PDMS/ZnO NWs NCFs.

## Growth of ZnO nanowire (ZnO NW) arrays

The preparation of ZnO NWs grown on a silicon substrate has been previously reported in our works.<sup>1-3</sup> In this present work, glass substrates are used instead of silicon substrates. First, microscope glass slides purchased from Sigma Aldrich are cut into 2.5 cm × 2.5 cm pieces and carefully cleaned with ethanol; the cleaned surface promotes nucleation and the growth of materials. A seed layer is prepared by depositing 300 μL of 0.37 M zinc acetate dehydrate ( $\text{Zn}(\text{CH}_3\text{COO})_2 \cdot 2\text{H}_2\text{O}$ , Sigma Aldrich, 99.999%) sol on the glass substrate using spin-coating. The as-prepared seed layer is placed in an oven at 540 °C for 1 h, promoting the crystallization of the seed layer. Subsequently, the substrate containing the seed layer is held using a Teflon sample holder with a 45° tilt angle. Meanwhile, a mixture of 100 mL of zinc nitrate hexahydrate ( $\text{Zn}(\text{NO}_3)_2 \cdot 6\text{H}_2\text{O}$ , Sigma Aldrich, >99.00%) and 100 mL of hexamethylenetetramine ( $\text{C}_6\text{H}_{12}\text{N}_4$ , Sigma Aldrich, >99.00%) of 25 mM concentration are preheated at 90 °C on a hot plate. Then, the sample is immersed in the solution bath maintained at 90 °C for 2 h. After the growth reaction, the sample is carefully rinsed with deionized water and dried with a nitrogen stream, then stored in a plastic container.

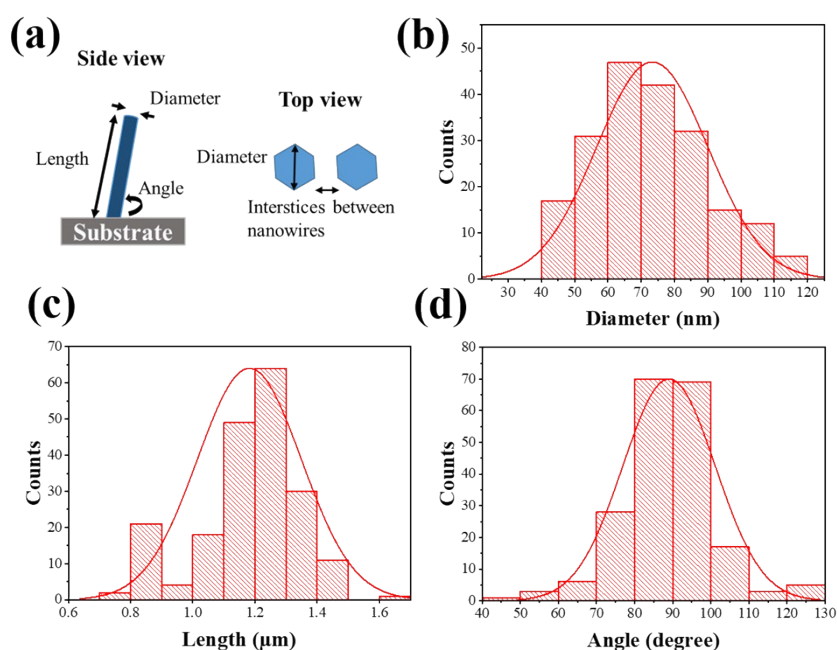


**Fig. S1.** Statistical analysis of the morphology of ZnO NWs. (a) Schematic of the dimensions measured from SEM images, (b) diameter ( $73 \pm 16$  nm), (c) length ( $1.2 \pm 0.17$  μm), and (d) angle ( $89 \pm 12$  °). Counted number = 200.

### Total effective surface area

From **Fig. S2**, there are 78 nanowires in an area of  $1 \mu\text{m}^2$ . Assuming that each nanowire is a cylinder, the total surface area for a nanowire on the substrate is calculated as:

$$S = \pi r^2 + 2\pi rL$$

in which  $r$  and  $L$  represent the radius and length of a nanowire which are 36.5 nm and 1.2  $\mu\text{m}$ , respectively. Thus, the total effective surface area of ZnO NWs in an area of  $1 \mu\text{m}^2$  is 21.79  $\mu\text{m}^2$ .

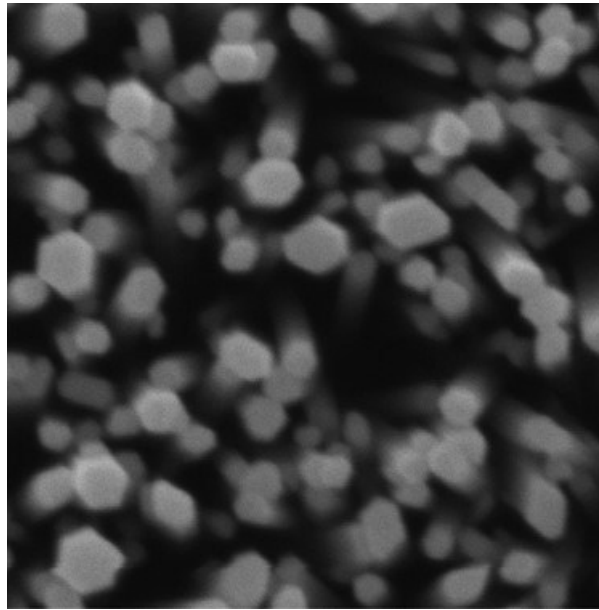


**Fig. S2.** Top-view SEM image of ZnO NW in an area of  $1 \mu\text{m}^2$ .

### Inverted LeCaRI

To confirm that oligomers infiltrate the interstices between NWs via capillarity, we conduct an inverted infiltration experiment to eliminate the effect of gravity. The substrate containing ZnO NW arrays is placed on top of a PDMS elastomer in which the ZnO NW arrays are brought into a conformal contact with the PDMS elastomer for 10 seconds to induce the transfer of uncross-linked and mobile oligomer chains from the elastomer network into the interstices of the ZnO NW arrays. Finally, the infiltrated ZnO NW arrays are heated to 80 °C for 1 h to cure the unreacted chains transferred into the interstices of ZnO NW arrays. The schematic illustration and SEM images showing the inverse LeCaRI process to fabricate nanocomposite films with vertically aligned ZnO NWs via inverse LeCaRI is shown in **Fig. S3**.

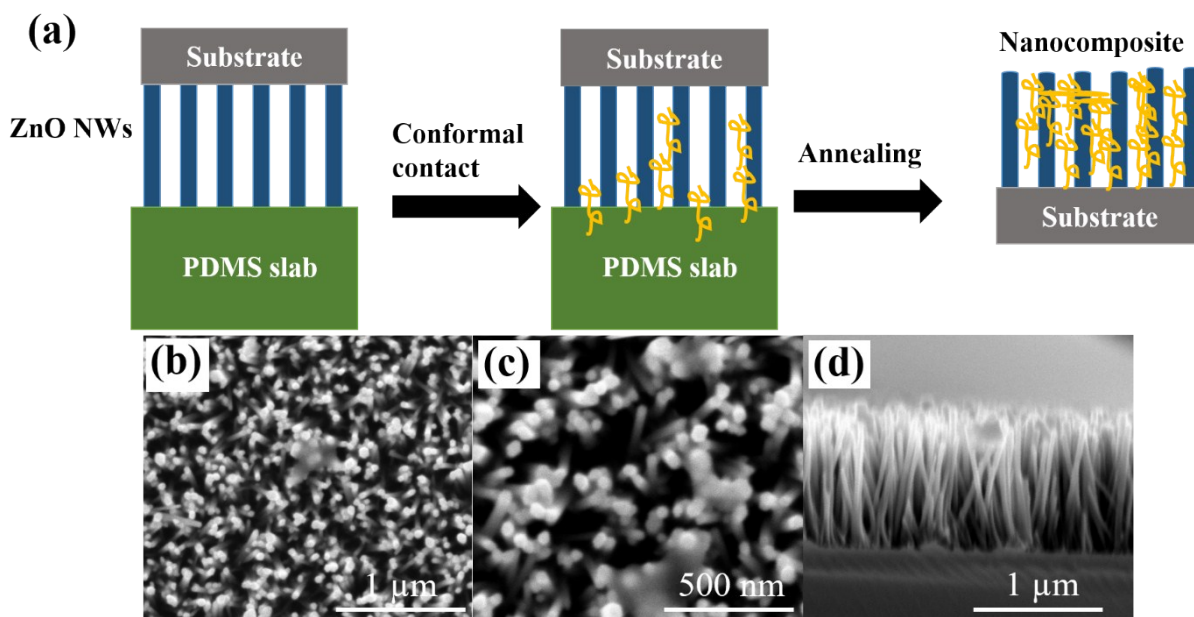


**Fig. S3.** (a) Schematic illustration showing the inverted LeCaRI process to fabricate nanocomposite films with vertically aligned ZnO NWs. For clarity, schematic illustrations are not drawn to scale. (b) and (c) Top-view SEM images at different magnifications, and (d) side-view SEM image of NCF-10s@RT produced via inverted LeCaRI.

### Optical microscope observation

The surface of ZnO NW arrays before and after infiltration are captured by using a Leica DM LM microscope with a modular design connected with a high-quality video camera (Olympus SC30). Images were taken using a 50× long working distance objective. The images are taken and collected by using the Stream Start software. The optical microscope images show that after infiltrating, the surface of the ZnO NW arrays is not significantly changed, the surface becomes more homogenous due to filling of the interstices and voids between nanowires, as shown in **Fig. S4**.

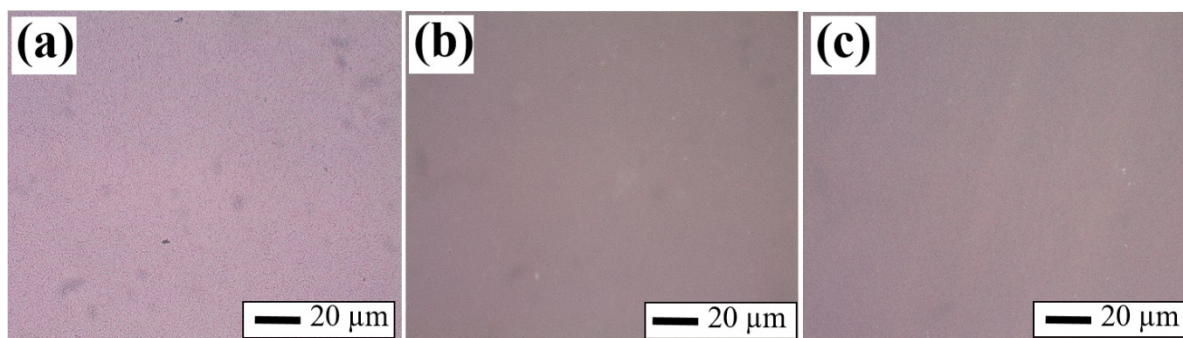


**Fig. S4.** Optical microscope images of ZnO NWs, NCFs-10s@RT, and NCFs-24h@150 °C.

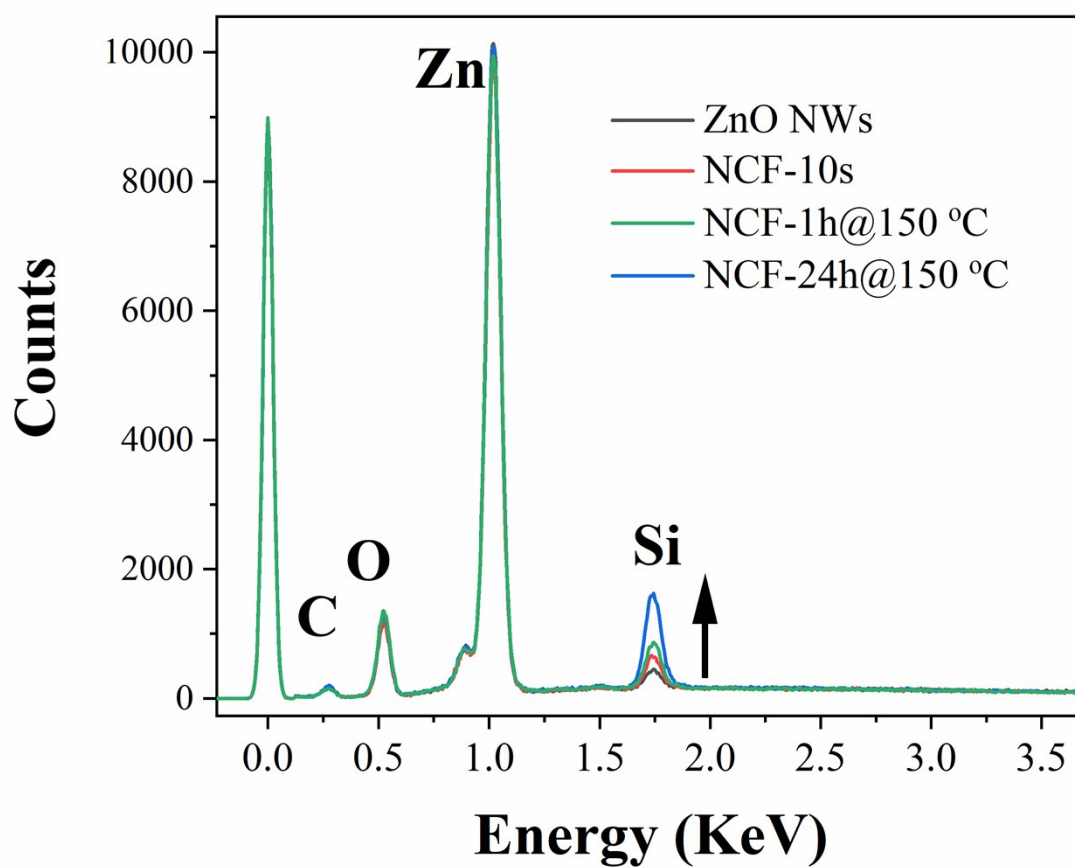


**Fig. S5.** EDS profiles of ZnO NWs and nanocomposite films.

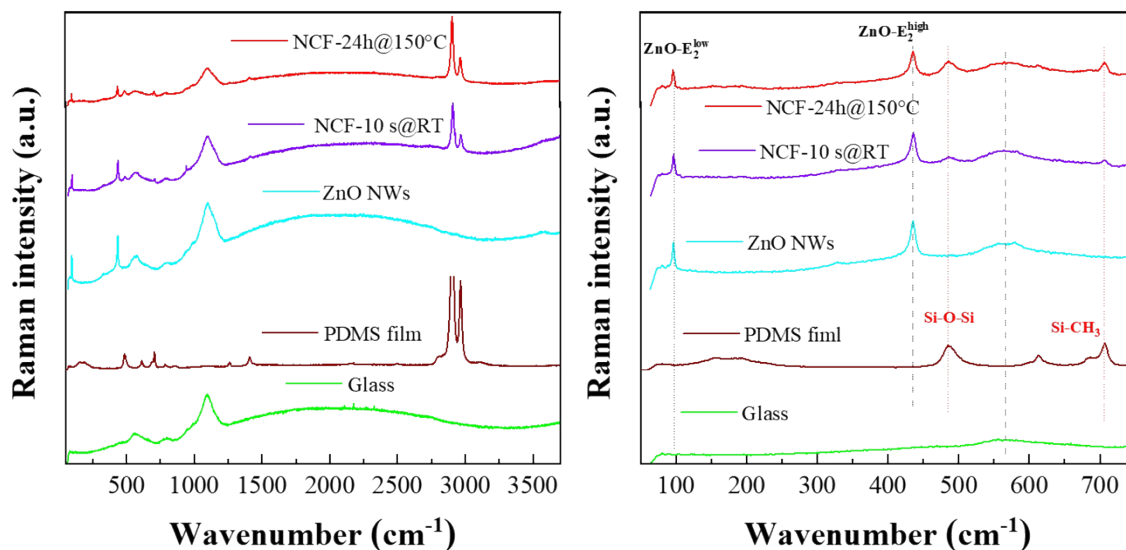


**Fig. S6.** Raman spectra of glass slide, ZnO NWs, PDMS film, NCF-10s@RT, and NCF-24h@150 °C.

Raman scattering spectroscopy is used to confirm the presence of PDMS oligomers in the NCFs. The Raman spectra are taken in the range of 50-3700  $\text{cm}^{-1}$ . **Fig. S6** shows that besides the typical Raman peaks for ZnO NWs, there are peaks associated with Si-O-Si symmetric stretching ( $488 \text{ cm}^{-1}$ ), Si-CH<sub>3</sub> symmetric rocking ( $687 \text{ cm}^{-1}$ ), CH<sub>3</sub> symmetric stretching ( $2907 \text{ cm}^{-1}$ ), and CH<sub>3</sub> asymmetric stretching ( $2965 \text{ cm}^{-1}$ ) of PDMS.<sup>4, 5</sup> The right side is the spectra taken between 50-750  $\text{cm}^{-1}$  for more detailed analysis. This result again confirms the presence of PDMS oligomer chains in the NCFs upon LeCaRI.

## References

1. T. Demes, C. Ternon, F. Morisot, D. Riassetto, M. Legallais, H. Roussel and M. Langlet, *Appl. Surf. Sci.*, 2017, **410**, 423-431.
2. T. Demes, C. Ternon, D. Riassetto, V. Stambouli and M. Langlet, *J. Mater. Sci.*, 2016, **51**, 10652-10661.
3. T. Demes, C. Ternon, D. Riassetto, H. Roussel, L. Rapenne, I. Gélard, C. Jimenez, V. Stambouli and M. Langlet, *J. Phys. Chem. Solids*, 2016, **95**, 43-55.
4. S. C. Bae, H. Lee, Z. Lin and S. Granick, *Langmuir*, 2005, **21**, 5685-5688.
5. R. Cuscó, E. Alarcón-Lladó, J. Ibáñez, L. Artús, J. Jiménez, B. Wang and M. J. Callahan, *Phys. Rev. B*, 2007, **75**.